

BEHAVIOR OF BUBBLES IN GLASS MELTS UNDER EFFECT OF THE GRAVITATIONAL AND CENTRIFUGAL FIELDS

LUBOMÍR NĚMEC, VLADISLAVA TONAROVÁ

Laboratory of Inorganic Materials,
Joint Workplace of the Institute of Chemical Technology Prague and the Institute of Inorganic Chemistry ASCR,
Technická 5, 166 28 Prague, Czech Republic

E-mail: nemece@iic.cas.cz

Submitted March 21, 2005; accepted June 23, 2005

Keywords: Glass refining, Bubbles, Modelling, Centrifugal forces

Bubble removing during glass melting may be a slow process if only the gravitational force determines its rate. The chemical refining mostly supports the bubble growth and accelerated rising of growing bubbles through viscous melt. Other forces can be as well applied to enhance bubble separation from the melt as is the centrifugal force, surface forces or melt oscillations due to supersonic waves, e.g. The increasing effort for advanced melting principles during last period restored interest in bubble separation by centrifugal force. This work brings derivation of relations governing the one and multicomponent bubble behavior in a rotating cylinder. The mass transfer between the bubble and melt is taken into account, both discontinual and continual regimes of the cylinder are considered. The derived equations indicate a relatively complicated bubble behavior in the centrifugal field as the bubble separation velocity may be increased by the centrifugal force but the bubble growth by gas diffusion may be suppressed. The parametric study of the problem using appropriate glass and refining data is needed to appreciate the process properly.

INTRODUCTION

Bubbles are removed from glass melts mostly by a separation process. Alternative mechanism - removing multicomponent bubbles by dissolution - requires extremely low concentrations of gases in the melt or high pressures. Glass melts, however, are saturated by gases coming from the decomposition of raw materials and consequently, bubble growth during the melting process is preferred to their dissolution. That is why refining agents are added into glass batch or lowered pressure is applied to promote bubble growth. The external force separating bubbles from melt is naturally the buoyancy force of the gravitational field which may be supported by bubble growth due to refining agents, by glass saturation by rapidly diffusing gases [1] or by reduced pressure [2-4]. However, also supersonic waves [5], surface forces and centrifugal force may be used to evoke or accelerate the bubble separation rate. The potentially feasible arrangement of the refining in the centrifugal field assumes treating the glass melt in a rotating cylinder under proper temperature and melt flow regime. The effect of both gravitational and centrifugal forces influences however the pressure inside of melt and consequently, the bubble growth or dissolution in the melt is affected. The goal of this paper is to present relations describing behavior of a bubble containing only gas released by the refining agent (refining gas) or behavior of a multicomponent bubble under simulta-

neous effect of gravitational and centrifugal fields and to discuss effect of melting conditions on the bubble separation.

THEORETICAL

Bubble growth or dissolution in simultaneous gravitational and centrifugal fields

A bubble containing pure gas (refining gas - usually oxygen, sulfur dioxide or mixture of both) or mixture of gases is considered located in a rotating vertical cylinder. The glass flows from upper part of cylinder to the bottom. The positive directions of movement are towards the cylinder bottom and to its periphery as is apparent from figure 1a, while the shapes of melt level at medium and high angle velocities are presented in figure 1b. If only refining gas is considered, its effect is assumed decisive for bubble interaction with the melt. Under effect of the gravitational field only, the bubble will move upwards. For a single bubble containing only the refining gas, the following simplified equation is valid under constant temperature and low hydrostatic pressure [6]:

$$\frac{da}{d\tau} = \frac{0.381RTD_R^{2/3}\rho^{1/3}g^{1/3}}{M_R\eta^{1/3}p_t}(c_{Rb} - c_{Ra}) \quad (1)$$

where a is the bubble radius, D_R and M_R are the diffusion coefficient and molecular mass of the refining gas,

c_{Rb} and c_{Ra} are the mass concentrations of the refining gas in the bulk glass and on the bubble surface, p_t is the total pressure and ρ and η are the glass density and viscosity.

It holds for c_{Ra} :

$$c_{Ra} = L_R p_t \quad (2)$$

where L_R is the physical solubility of the refining gas at normal pressure.

Equation (1) may be written as:

$$\frac{da}{d\tau} = \frac{0.381RTD_R^{2/3}\rho^{1/3}g^{1/3}}{M_R\eta^{1/3}} \left(\frac{c_{Rb}}{p_t} - L_R \right) \quad (3)$$

The derivation of the expression $da/d\tau$ under simultaneous effect of gravitational and centrifugal fields needs to define the centrifugal velocity. Analogically to Stokes' velocity, the coefficient of resistance against movement of fine bubbles is $24/Re$ and for \bar{v} we have:

$$4/3\pi a^3 (\rho_{gas} - \rho_{glass}) \omega^2 r = 6\pi a \bar{v} \eta \quad (4)$$

$$\bar{v} = \frac{dr}{d\tau} = -\frac{2\omega^2 r \rho a^2}{9\eta} \quad (5)$$

The gravitational acceleration in equation (5) is replaced by the centrifugal one, $\omega^2 r$, where r is the radial distance and ω is the angle velocity. $\rho = \rho_{glass} \gg \rho_{gas}$ is supposed. Equation (5) has thus the form analogical to the Stokes' equation. The total bubble velocity in the cylinder is then given by:

$$v_{bub} = (v^{\uparrow 2} + \bar{v}^2)^{1/2} = \left[\left(-\frac{2g\rho a^2}{9\eta} \right)^2 + \left(-\frac{2\omega^2 r \rho a^2}{9\eta} \right)^2 \right]^{1/2} \quad (6)$$

where v^{\uparrow} is the Stokes' bubble rising velocity. The value of v_{bub} is then:

$$v_{bub} = \frac{2\rho a^2}{9\eta} (g^2 + \omega^4 r^2)^{1/2} \quad (7)$$

As pressure in the bubble changes both with bubble depth and its distance from the cylinder center, the pressure changes should be expressed from the derivative of the Gay Lussac's equation. The bubble volume $4/3\pi a^3$ is taken into account:

$$\frac{dp_t}{d\tau} 4/3\pi a^3 + p_t 4\pi a^2 \frac{da}{d\tau} = \frac{RT}{M_R} \frac{dm}{d\tau} + \frac{mR}{M_R} \frac{dT}{d\tau} \quad (8)$$

The total pressure inside of cylinder is:

$$p_t = p_{ex} + \rho gh + \frac{\rho \omega^2 r^2}{2} + \frac{2\sigma}{a} \quad (9)$$

where p_{ex} is the external pressure and h is the bubble

depth under glass level. For $dp_t/d\tau$ it holds:

$$\frac{dp_t}{d\tau} = \rho g \frac{dh}{d\tau} + \rho \omega^2 r \frac{dr}{d\tau} - \frac{2\sigma}{a^2} \quad (10)$$

As $dr/d\tau = \bar{v}$ and $dh/d\tau$ is the Stokes' bubble rising velocity, we have:

$$\frac{dp_t}{d\tau} = -\frac{2g^2 \rho^2 a^2}{9\eta} - \frac{2\omega^4 r^2 \rho^2 a^2}{9\eta} - \frac{2\sigma}{a^2} \quad (11)$$

The total amount of gas inside the bubble is given by:

$$m = \frac{4/3\pi a^3 p_t M_R}{RT} \quad (12)$$

After expressing the term $4/3\pi a^3 dp_t/d\tau$ by means of equation (11) and the term $mR/M_R dT/d\tau$ by using equation (12), the resulting equation for $da/d\tau$ has the form:

$$\begin{aligned} & -\frac{8\pi\rho^2 a^5}{27\eta} (g^2 + \omega^4 r^2) - \frac{8\pi\sigma a}{3} + \\ & + 4\pi a^2 p_t \frac{da}{d\tau} = \frac{RT}{M_R} \frac{dm}{d\tau} + \frac{4/3\pi a^3 p_t}{T} \frac{dT}{d\tau} \end{aligned} \quad (13)$$

The following simplifying assumptions will be now accepted:

- variations of the hydrostatic pressure will be neglected: (the term $\frac{8\pi\rho^2 a^5}{27\eta} g^2$)
- variations of surface forces will be neglected: (the term $\frac{8\pi\sigma a}{3}$)
- temperature will be constant: ($dT/d\tau = 0$)

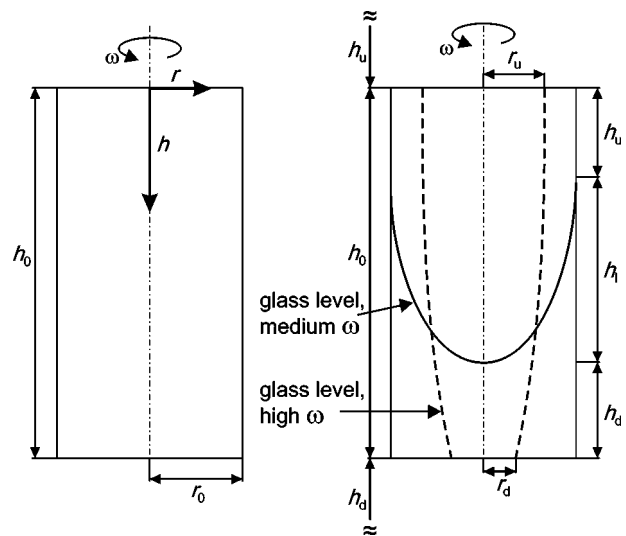


Figure 1. The orientation of coordinates and sizes of the rotating cylinder (left). The shapes of melt level at medium and high cylinder angle velocities (right).

The resulting equation after rearrangement has the form:

$$\frac{da}{d\tau} = \frac{RT}{4\pi M_R p_i a^2} \frac{dm}{d\tau} + \frac{2\omega^4 r^2 \rho^2 a^3}{27\eta p_i} \quad (14)$$

where the first term on the right hand side of equation (14) represents the change of bubble size by gas diffusion and the second one the effect of centrifugal force.

When applying equation for $dm/d\tau$, the complete acceleration involved in parentheses of equation (7) in form of $(g^2 + \omega^4 r^2)^{1/2}$ should be used. The resulting equation has the form:

$$\begin{aligned} \frac{da}{d\tau} = & \frac{0.381RTD_R^{2/3} \rho^{1/3}}{M_R \eta^{1/3}} (g^2 + \omega^4 r^2)^{1/6} \left(\frac{c_{Rb}}{p_i} - L_R \right) + \\ & + \frac{2\omega^4 r^2 \rho^2 a^3}{27\eta p_i} \end{aligned} \quad (15)$$

The total pressure when neglecting the hydrostatic pressure and surface force is:

$$p_i = p_{ex} + \rho\omega^2 r^2 / 2 \quad (16)$$

To solve equation (15), the relation for development of r is needed: As $dr/d\tau = \bar{v}$, equation (5) is used simultaneously with (15-16).

The member expressing changes of hydrostatic pressure should be taken into account in tall cylinders, the completed equation (15) is then:

$$\begin{aligned} \frac{da}{d\tau} = & \frac{0.381RTD_R^{2/3} \rho^{1/3}}{M_R \eta^{1/3}} (g^2 + \omega^4 r^2)^{1/6} \left(\frac{c_{Rb}}{p_i} - L_R \right) + \\ & + \frac{2\omega^4 r^2 \rho^2 a^3}{27\eta p_i} + \frac{2g^2 \rho^2 a^3}{27\eta p_i} \end{aligned} \quad (17)$$

The total pressure is:

$$p_i = p_{ex} + \rho gh + \frac{\rho\omega^2 r^2}{2} \quad (18)$$

As for h expression, the Stokes' equation is valid:

$$v^\uparrow = \frac{dh}{d\tau} = -\frac{2g\rho a^2}{9\eta} \quad (19)$$

When solving the bubble movement in a rotating cylinder with quiescent glass (no throughflow), the bubble trajectory is obtained by simultaneous solution of equations (5) and (17-19).

If the bubble is multicomponent, the mass transfer of all present gases will play a role. The following equations for behavior of a multicomponent bubble in the gravitational and centrifugal fields are valid analogically to relations derived for a bubble containing pure gas [6]:

$$\begin{aligned} \frac{da}{d\tau} = & \frac{0.381RT \rho^{1/3} (g^2 + \omega^4 r^2)^{1/6}}{\eta^{1/3} p_i} \sum_{i=1}^n \frac{D_i^{2/3}}{M_i} (c_{ib} - L_i p_i) + \\ & + \frac{2g^2 \rho^2 a^3}{27\eta p_i} + \frac{2\omega^4 r^2 \rho^2 a^3}{27\eta p_i} \end{aligned} \quad (20)$$

$$\frac{dp_i}{d\tau} = \frac{1.143RT \rho^{1/3} (g^2 + \omega^4 r^2)}{\eta^{1/3} a} \frac{D_i^{2/3}}{M_i} (c_{ib} - L_i p_i) - \frac{3p_i}{a} \frac{da}{d\tau} \quad (i=1, 2 \dots n-1) \quad (21)$$

$$p_i = \sum_{i=1}^n p_i \quad (22)$$

When solving behavior of the multicomponent bubble, equations (5), (18-19) and (20-22) have to be involved.

The level shape in a rotating cylinder

The level is formed according to pressure field inside glass melt evoked by the centrifugal force. The pressure due to centrifugal force is given, according to equation (18), by the expression $\rho\omega^2 r^2/2$, i.e. the pressure grows towards the cylinder mantle and its growth should be equilibrated by the increase in hydrostatic pressure if the liquid would be quiescent. The level shape is to be calculated from the equilibrium between both pressures:

$$h = \frac{\omega^2 (r_o^2 - r^2)}{2g} \quad (23)$$

where r_o is the cylinder radius.

The parabolic shapes of the glass level are obvious from figure 1b. At a very high angle velocity, the melt will be stuck on the walls and only upper part of the parabolic level shape will be present (see dashed curves). If the continual regime is set up, the liquid entering the cylinder should be distributed to the upper part of the cylinder mantle.

The total height of the rotation paraboloid ranging from the intersection of its mantle with cylinder wall to cylinder top, h_i , determines the actual shape of the melt level in the cylinder. h_i is obtained from equation (23) at $r = 0$:

$$h_i = \frac{\omega^2 r_o^2}{2g} \quad (24)$$

If $h_i \leq h_o$, the full level profile establishes in figure 1b and the total cylinder height, h_o , can be divided into three parts: the upper part, h_u , is without contact with

melt, h_l is appropriate height of the paraboloid level and h_d is the lower part containing melt in the full cylinder horizontal profile. Assume that the total volume of melt in the cylinder is constant, V . The values of h_u and h_d are then given by:

$$h_u = h_o - \frac{\omega^2 r_o^2}{4g} - \frac{V}{\pi r_o^2} \quad (25)$$

$$h_d = \frac{V}{\pi r_o^2} - \frac{\omega^2 r_o^2}{4g} \quad (26)$$

At higher cylinder angle velocities, $h_l > h_o$, and the dashed level profile in figure 1b is valid. The values of h_u and h_d are out of the cylinder and cylinder should be partially covered in its upper part to prevent melt from splashing from it. The melt level intersects the cylinder cap and bottom at radial distances r_u and r_d (see figure 1b). The appropriate values are given by following equations:

$$r_u = \left(\frac{gh_o}{\omega^2} + r_o^2 - \frac{V}{\pi h_o} \right)^{1/2} \quad (27)$$

$$h_u = \frac{\omega^2 (r_o^2 - r_u^2)}{2g} \quad (28)$$

$$r_d = \frac{[\omega^2 r_u^2 - 2gh_o]^{1/2}}{\omega} \quad (29)$$

$$h_d = \frac{\omega^2 r_u^2}{2g} - h_o \quad (30)$$

The bubble trajectory in a rotating cylinder

The angle velocity is low and the level curvature is negligible

If the glass is flowing downwards by a plug flow and the constant glass velocity has the value v_h , equation (19) has the form:

$$\frac{dh}{d\tau} = v_h - \frac{2g\rho a^2}{9\eta} \quad (31)$$

In the cylinder with a parabolic glass velocity profile, the bubble local vertical velocity gives equation (32) where the local downward velocity of glass is given by the first and second term on the right hand side of this equation:

$$\frac{dh}{dt} = 2\bar{v}_h - \frac{2\bar{v}_h}{r_o^2} r^2 - \frac{2g\rho a^2}{9\eta} \quad (32)$$

where \bar{v}_h is the average glass velocity. Equations (31-32) may be used only at very low ω .

The expected behavior of bubbles in the combined gravitational and centrifugal field is rather complicated as considerable pressure changes during the process will influence bubble size through both gas compressibility and gas transfer between bubbles and melt. If the bubble with glass enters the rotating cylinder close to its periphery, the instant pressure jump up will occur, leading to bubble compression and slowing down the bubble growth rate, which fact may evoke even dissolution. The approximate initial bubble radius may be calculated by taking into account only the bubble compression. Consequently, the initial bubble growth or dissolution rate is determined. The initial bubble radius results from equation:

$$a_o = a'_o \left(\frac{P_{ex}}{P_{ex} + \rho\omega^2 r^2 / 2} \right)^{1/3} \quad (33)$$

where a'_o is the radius of bubble just before entering the rotating cylinder.

Subsequently, the trajectory of the bubble is calculated leading to the cylinder centre and mostly upwards. As pressure decreases with radial bubble movement and later also with bubble rising, the increase of bubble growth rate along the bubble trajectory will be promoted (the second and third members in equation (17)) but the simultaneous decrease in r in the second term will slow down this tendency. Simultaneously, the concentration difference in the first term grows supporting bubble growth by diffusion. At $r = 0$, the effect of the centrifugal field disappears in the first and second terms. At higher values of angle velocity, ω , the contribution to the bubble growth rate in the second term grows too, but the increase in the total pressure reduces this contribution. In addition, the high value of the total pressure at high ω may lead to a considerable slowing down the bubble growth rate by diffusion as it is obvious from the concentration difference in the first term of equation (17).

The problem of the criterion of refining remains to be solved. The bubble may be refined when reaches glass level, cylinder centre (where bubble coalescence with subsequent rapid rising is assumed) or as soon as it attains the same rising velocity as is the negative value of v_h before or just at the cylinder bottom. This expected behavior does not provide an unambiguous picture of bubble refining under influence of the centrifugal force. A numerical examination of the process is therefore necessary.

The rotation velocity is high and the melt occupies mostly the cylinder mantle

Figure 2 presents the detailed schematic picture of the level shape and melt velocities at higher angle

velocities. Glass melt is distributed by a circular distributor to the upper part of the cylinder mantle so as the level shape on the contact between melt and cylinder will not be sharp but round. The melt is flowing down and the parabolic vertical velocity profile is assumed between the cylinder mantle and curved melt level, with maximum on the level. As the flow profile extends downwards, the radial velocity component should be present. As it is obvious from figure 2, the melt velocity in the point A is tangential to the melt surface. For angle α we have:

$$\operatorname{tg} \alpha(A) = \frac{v_{h \max}}{v_{r \max}} = -\frac{\omega^2 r_A}{g} \quad (34)$$

where $v_{h \max}$ is the maximum vertical velocity and $v_{r \max}$ is the maximum radial velocity of melt in the mentioned point on the glass level. The value of the average vertical melt velocity is given by the melt throughflow in the flow profile:

$$\dot{V} = \pi \bar{v}_h (r_o^2 - r_A^2) \quad (35)$$

where \bar{v}_h is the average vertical (axial) velocity component.

The equation expressing the parabolic vertical velocity profile in the ring $r_o - r_A$ is given by:

$$v_h = v_{h \max} - \frac{v_{h \max}}{(r_o - r_A)^2} (r - r_A)^2 \quad (36)$$

and relation between \bar{v}_h and $v_{h \max}$ in the ring $r_o - r_A$ is given by:

$$\bar{v}_h = v_{h \max} - v_{h \max} \frac{3r_o^2 - 2r_o r_A - r_A^2}{6(r_o^2 - r_A^2)} \quad (37)$$

Taking into account equations (35-37), the vertical melt velocity distribution in the horizontal plane containing the point A is given by:

$$v_h = \frac{6\dot{V}}{\pi(3r_o^2 + 2r_o r_A - 5r_A^2)} \left[1 - \frac{(r - r_A)^2}{(r_o - r_A)^2} \right] \quad (38)$$

To be informed about the radial velocity distribution, let us define its maximum value by means of equations (34) and (38) ($r = r_A$ in equation (38)):

$$v_{r \max} = -\frac{6\dot{V}g}{\pi\omega^2 r_A (3r_o^2 + 2r_o r_A - 5r_A^2)} \quad (39)$$

The flow profile expands in downward direction and the development of the radial distribution should be estimated. The vertical glass velocity should be at first expressed as a function of h . Taking into account equation (23) for $r = r_A$, equation (38) may be expressed as:

$$v_h(h) = \frac{6\dot{V}}{\pi \left[3r_o^2 + 2r_o \left(\frac{\omega^2 r_o^2 - 2gh}{\omega^2} \right)^{1/2} - 5 \left(\frac{\omega^2 r_o^2 - 2gh}{\omega^2} \right) \right]} \left\{ 1 - \frac{\left[r - \left(\frac{\omega^2 r_o^2 - 2gh}{\omega^2} \right)^{1/2} \right]^2}{\left[r_o - \left(\frac{\omega^2 r_o^2 - 2gh}{\omega^2} \right)^{1/2} \right]^2} \right\} \quad (40)$$

The values of v_r may be obtained from the continuity equation in cylindrical coordinates:

$$\frac{1}{r} \frac{\partial}{\partial r} (rv_r) + \frac{\partial v_h}{\partial h} = 0 \quad (41)$$

The boundary conditions for solution of equation (41), where $\partial v_h / \partial h$ is obtained from equation (40), are: $v_r = 0$ if $r = r_o$ and v_r comes from equation (39) if

$$r = r_A = \left(\frac{\omega^2 r_o^2 - 2gh}{\omega^2} \right)^{1/2}$$

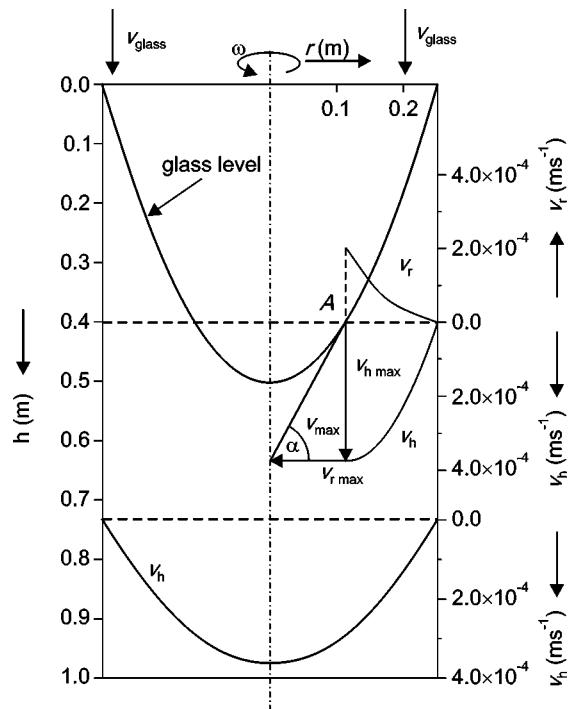


Figure 2. The schematic picture of the vertical central section through the rotating cylinder with calculated shape of the level and distribution of both vertical and radial melt velocities at $h = 0.4$ m and $h > 0.5$ m.

Equation (39) is not valid at $r_A = 0$ and simultaneously $r = 0$. Nevertheless, the mentioned fact is not considered significant for determination of bubble trajectories. Taking into account equations (40) and (41) with the above mentioned boundary conditions, the radial velocity distribution may be calculated. The calculated velocity distribution of v_h and the estimated distribution of v_r for the standard case are presented in figure 2. When calculating the bubble trajectory in the cylinder, the resulting bubble vertical velocity is the sum of Stokes' velocity (equation (19)) and v_h from equation (40), and the resulting bubble radial velocity is given by the sum of the bubble radial velocity given by equation (5) and the melt radial velocity coming from solution of equation (41).

As soon as glass melt with bubbles reaches the region below the lowest point of the melt level, the parabolic velocity profile across the entire refining cylinder is assumed (see equation (32)).

Melt flowing out of the rotating cylinder under continual regime

The flow out can cause a problem at higher rotation velocities. Two arrangements are possible. The first regime assumes the flow out through the bottom center, however, the outflow will rotate with the cylinder and melt may produce air bubbles or cords after contact with quiescent glass. The second regime assumes the melt flows out by exits in the cylinder mantle close to the bottom [7]. The short exit tubes are assumed turned along the cylinder mantle so that the melt flows out against the direction of rotation. The desired situation will set up when the absolute value of the average outflow melt velocity is identical to the velocity of the rotating mantle. If the radius of the exit tube is R , the equivalence has the form:

$$(r_o + R)\omega = \left(\rho gh + \frac{\rho \omega^2 r_o^2}{2} \right) R^2 / 8\eta l_e \quad (42)$$

where the member on the left hand side designates the cylinder circumference velocity, v_ω , and the right hand side brings the average glass velocity leaving the exit tube, v_{glass} . l_e is the effective length of the exit tube.

RESULTS OF CALCULATIONS AND DISCUSSION

The case of pure oxygen bubble was selected to show the fundamental tendencies of bubble behavior in the centrifugal field. The standard case involved glass melt at 1300°C having density 2300 kg/m³ and viscosity 60 Pas. To calculate the vertical and to estimate the radial velocity distributions of the melt, the average verti-

cal glass velocity was selected corresponding to removing the critical bubble having initial radius $a_0 = 5 \times 10^{-5}$ m and exhibiting the growth rate $a = 5 \times 10^{-7}$ m/s in the cylinder without rotation. The value of the critical vertical glass velocity for the cylindrical channel having height 1 m and radius 0.25 m was 1.805×10^{-4} m/s and throughflow of the channel was 3.544×10^{-5} m³/s. When calculating the melt level in the rotating cylinder, the angle velocity 12.53 s^{-1} was used. The lowest point of the melt level curvature at this angle velocity lays at $h = 0.5$ m (see figure 2). The melt level and the appropriate melt velocities, v_h and v_r , in the horizontal plane $h = 0.4$ m and $h > 0.5$ m are plotted in figure 2. Three initial values of bubble growth rates were chosen for further calculations corresponding to slow, medium and rapid refining when taking into account the experimetal experience, namely 1×10^{-7} m/s, 5×10^{-7} m/s and 1×10^{-6} m/s. The distinct sensibility of the bubble growth rate to angle velocity and bubble radial position is expected. Figure 3 presents the dependence between the oxygen concentration gradient on the bubble surface and the cylinder angle velocity; the growing pressure in the bubble due to the centrifugal force is presented too. As pressure grows inside the bubble, the concentration gradient decreases according to equation (3) and attains negative values at higher angle velocities, i.e. the bubble growth transforms to bubble dissolution. This fact is also obvious from figure 4 presenting the bubble growth rates as a function of angle velocity for the same cases as in figure 3. However, the initial increase in bubble growth rates is apparent as a consequence of growing bubble moving velocity which reduces the thickness of the diffusion layer on the bubble boundary (this fact is demonstrated by the member $g^2 + \omega^4 r^2$ in equations (7), (15) and (17)). At higher angle velocities, the bubble

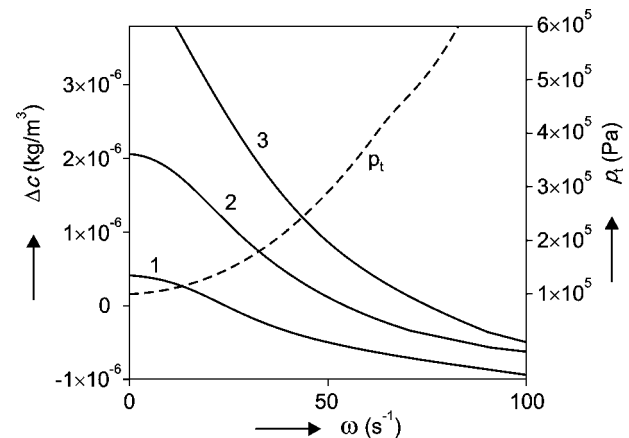


Figure 3. The dependence between the oxygen concentration difference on the bubble boundary and the cylinder angle velocity ω at different initial bubble growth rates. $r = r_0 = 0.25$ m, 1: $da/d\tau (\omega = 0) = 1 \times 10^{-7}$ m/s, 2: $da/d\tau (\omega = 0) = 5 \times 10^{-7}$ m/s, 3: $da/d\tau (\omega = 0) = 1 \times 10^{-6}$ m/s.

growth rate decreases to even negative values due to growing pressure inside bubbles. The optimum angle velocity may be therefore found from the point of view of bubble growing. As it can be expected, higher initial bubble growth rates shift the actual zero value of the bubble growth rate in figure 4 to higher angle velocities. The high pressure in bubbles at considerable angle velocities may lead to a complete dissolution of bubbles containing pure gas. This fact may be potentially utilized for bubble removing by their dissolution in melt. Real bubbles, however, contain a mixture of gases and multicomponent bubbles need much higher angle velocities than bubbles of pure gas, as well as high temperatures, to dissolve completely.

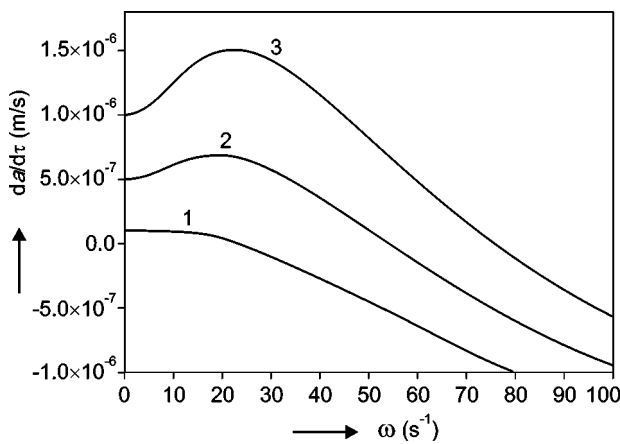


Figure 4. The dependence between the rate of change of bubble radius, $da/d\tau$, and the cylinder angle velocity ω at different initial bubble growth rates.

$r = r_0 = 0.25$ m, 1: $da/d\tau (\omega = 0) = 1 \times 10^{-7}$ m/s, 2: $da/d\tau (\omega = 0) = 5 \times 10^{-7}$ m/s, 3: $da/d\tau (\omega = 0) = 1 \times 10^{-6}$ m/s.

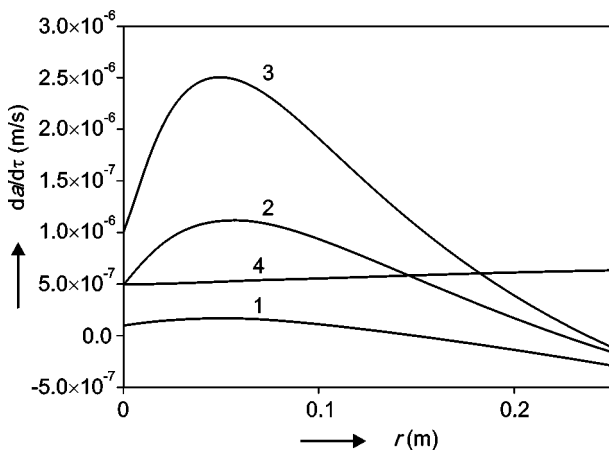


Figure 5. The dependence between the rate of change of bubble radius, $da/d\tau$, and the bubble distance from the center.

1: $\omega = 40$ s⁻¹, $da/d\tau (r = 0) = 1 \times 10^{-7}$ m/s; 2: $\omega = 60$ s⁻¹, $da/d\tau (r = 0) = 5 \times 10^{-7}$ m/s; 3: $\omega = 80$ s⁻¹, $da/d\tau (r = 0) = 1 \times 10^{-6}$ m/s; 4: $\omega = 10$ s⁻¹, $da/d\tau (r = 0) = 5 \times 10^{-7}$ m/s.

The influence of the radial distance on the bubble growth or dissolution is demonstrated in figure 5 for the same initial bubble growth rates as in figures 3-4. The constant cylinder rotation velocities were taken from cases 1-3 in figures 3-4, corresponding to a slow bubble dissolution close to the cylinder mantle. In cases 1-3, the bubble grew along the substantial part of the cylinder radius and a maximum was obvious in the region around $r = 0.05$ m (if melt is present) as a consequence of competition between decreasing pressure and decreasing bubble moving velocity. At relatively low angle velocities, only a slight influence of rotation on the mass transfer was obvious; the decreasing bubble moving velocity was here decisive (see curve 4 in figure 5).

Figure 6 presents the dependences between both velocities from equation (42), namely the plot of the cylinder circumference velocity, v_ω , and the average glass outflow velocity, v_{glass} , against cylinder angle velocity, ω . As it results from equation (42) and as it is obvious from figure 6 (see curve 1), the identity between absolute values of v_ω and v_{glass} may be attained at two values of ω . Especially the higher value of ω would be interesting with respect to high expected bubble separation velocities. However, the hydrodynamic resistance of the exit tube plays an important role when searching for acceptable refining parameters. The curve 2 in figure 6 presents the same dependence when increasing twice the effective length of the exit tube because of its curvature: the identity of both velocities may be expected at very high cylinder angle velocities. In addition, the glass outflow should be matched with refining ability of the cylinder. The very cautious examination of the cylinder regime and bubble behavior is therefore needed prior to applying the centrifugal refining.

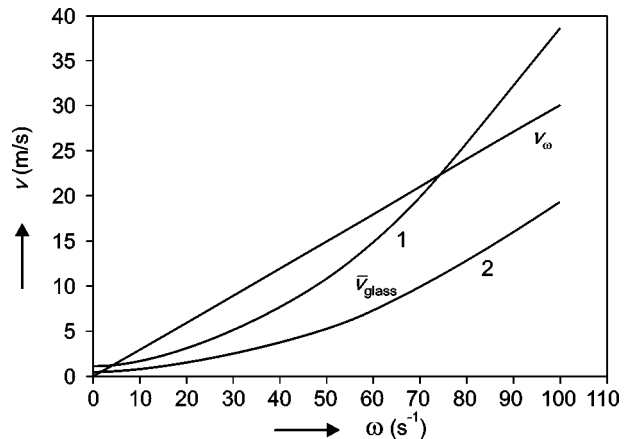


Figure 6. The dependence between the cylinder circumferential velocity, v_ω , average glass exit velocities, v_{glass} , and cylinder angle velocity.

1: v_{glass} at $l_e = 0.1$ m, 2: v_{glass} at $l_e = 0.2$ m.

The presented results involve bubble behavior in rotating cylinders under isothermal conditions. If temperature is not homogeneous, convective currents set up in the cylinder and complicate the both bubble interaction with melt and their trajectories. As temperature will be usually higher close to the cylinder mantle (external heating) and temperature gradients are smaller in the thinner glass layer, the mentioned problems will be less significant at higher rotation velocities.

CONCLUSIONS

The equations describing melt flow and bubble behaviour in the simultaneous gravitational and centrifugal fields were presented with the aim to evaluate the significance of the centrifugal force for glass refining. The application of centrifugal force on rotating both discontinual and continual cylinders leads to an increase in pressure and mostly to enhancement of mass transfer between bubbles and melt. At very high rotation velocities, the dissolution is dominating and complete dissolution of bubbles in melt may become the refining mechanism. However, the very high cylinder rotation velocities at relatively high temperatures are tentatively needed to accomplish the dissolution mechanism for multicomponent bubbles. When applying the bubble separation from the melt by bubble moving to phase boundary between melt and atmosphere, the bubble growth is preferred to accelerate the bubble separation rate. The value of the bubble growth rate depends in a complicated way on the both cylinder rotation velocity and bubble radial distance from the cylinder center. The increasing pressure decreases concentration difference on the bubble boundary and simultaneously the thickness of the bubble diffusion layer decreases due to growth of the bubble moving velocity. The maximum values of bubble growth rates obvious from their dependences on cylinder angle velocity or bubble radial distance are a consequence of the above mentioned influences. The effective setting up conditions for bubble removing in rotating spaces needs therefore a detailed parametrical study of the problem.

Acknowledgement

This study was a part of research programme IRP No. Z40320502 Design, synthesis and characterisation of clusters, composites, complexes and other compounds based on inorganic substances; mechanisms and kinetics of their interactions.

References

1. Beerkens R.: Proc. 7th Int. Conf. on Advances in Fusion and Processing of Glass III, Rochester NY, July 27-31, 2003.
2. Ross C. P.: Am.Ceram.Soc.Bull. 83, 8 (2004).
3. Kunkle G. E., Welton W.M., Schweninger R. L : US Pat. 4,738,938 (1988).
4. Kloužek J., Němec L., Ullrich J.: Glastechn.Ber.Glass Sci.Technol. 73, 329 (2000).
5. US Pat. 4,316,734.
6. Němec L., Kloužek J.: J.Non-Cryst.Solids 231, 152 (1998).
7. Kučera J.: Private communication.

CHOVÁNÍ BUBLIN VE SKELNÝCH TAVENINÁCH ZA PŮSOBENÍ GRAVITAČNÍHO A ODSTŘEDIVÉHO POLE

LUBOMÍR NĚMEC, VLADISLAVA TONAROVÁ

*Laboratoř anorganických materiálů,
společně pracoviště Vysoké školy chemicko-technologické
v Praze a Ústavu anorganické chemie AVČR,
Technická 5, 166 28 Praha*

Odstraňování bublin ze skelných tavenin separací je velmi pomalý proces, jestliže se uplatní pouze vztlaková síla. K urychlení procesu se používá většinou chemická cesta spočívající v uvolňování plynů z některých složek skla do taveniny a vedoucí k růstu bublin a jejich urychlenému vzestupu taveninou. Separace bublin od taveniny může být rovněž urychlena aplikací dalších sil, jako je síla odstředivá, povrchové síly nebo oscilace taveniny vyvolané ultrazvukovými vlnami. Zvýšený zájem o nová uspořádání tavicího procesu v poslední době oživil i problematiku odstraňování bublin v rotujících prostorech. Tato práce přináší odvození rovnic řídicích chování bublin ve skelné tavenině nacházející se v rotujícím vertikálním válci bez průtoku i s průtokem. Současně se předpokládá difúze plynů mezi bublinami a taveninou. Odvozené rovnice indikují poměrně složité chování bublin v odstředivém poli, neboť rychlost separace bublin od taveniny je ovlivňována protichůdnými faktory, zrychlením separační rychlosti bublin v důsledku odstředivého zrychlení a jejím zpomalením v důsledku klesajícího růstu bublin. Pro nalezení optimálních podmínek procesu je potřebná podrobnější parametrická studie využívající reálná data o skle a chování bublin ve skle.